

## Resistivity anomaly in the vicinity of a structural phase transition in $\text{La}_{1-x}\text{Sr}_x\text{MnO}_3$

P. Mandal, B. Bandyopadhyay, and B. Ghosh

*Saha Institute of Nuclear Physics, 1/AF Bidhannagar, Calcutta 700 064, India*

(Received 26 April 2001; published 16 October 2001)

The resistivity  $\rho$  has been measured up to 900 K in  $\text{La}_{1-x}\text{Sr}_x\text{MnO}_3$  ( $0 \leq x \leq 0.15$ ) single crystals to investigate the nature of charge transport phenomena both above and below the cooperative Jahn-Teller orbital-ordering temperature ( $T_{JT}$ ). At high temperatures above  $T_{JT}$ ,  $\rho$  is almost temperature independent for  $\text{LaMnO}_3$  whereas  $\rho$  exhibits a strong temperature dependence for  $x > 0$  samples. In the orbitally ordered state,  $\rho$  can be described well by a small-polaron hopping model with  $\rho(T) = \rho_0 \exp(E_p/kT)$ . We observe that both above and below  $T_{JT}$  the resistivity can be fitted with the same activation energy  $E_p$  but with different prefactor  $\rho_0$  for  $x > 0$  samples. Though  $\rho$  decreases monotonically with increasing doping concentration,  $E_p$  is almost independent of Sr concentration up to  $x = 0.10$  and then decreases rapidly above this value of  $x$ .

DOI: 10.1103/PhysRevB.64.180405

PACS number(s): 75.30.Et, 75.30.Vn, 71.70.Ej

The richness of the phase diagram of divalent doped colossal magnetoresistive (CMR) compounds  $R_{1-x}A_x\text{MnO}_3$  ( $R$ : rare-earth ions,  $A$ : divalent ions) is an outcome of intriguing competition between the ferromagnetic double exchange (DE) interaction and orbital/charge ordering. The parent compound  $\text{LaMnO}_3$  is an  $A$ -type antiferromagnetic (AFM) insulator in which  $d_{3x^2-r^2}$  and  $d_{3y^2-r^2}$   $e_g$  orbitals are alternately ordered in the  $ab$  plane due to the cooperative Jahn-Teller (JT) interaction. This particular orbital arrangement is responsible for strong ferromagnetic (FM) coupling in the  $ab$  plane and weak AFM coupling along the  $c$  axis which has been established in the remarkable experimental work by Wollan and Koehler.<sup>1</sup>

With the progress of hole doping, the DE interaction between  $\text{Mn}^{3+}$  and  $\text{Mn}^{4+}$  through electron transfer becomes prevalent. The coherent hopping of carriers with spin memory favors the FM metallic state and weakens the orbitally ordered AFM insulating state. Sr-doped  $\text{LaMnO}_3$  becomes FM at around  $x = 0.10$  and over a narrow range of doping around  $x = 0.125$  a sequence of transitions occur as a function of temperature due to the competition between DE and other interactions favoring charge localization.<sup>2-8</sup> As a result metalliclike conductivity ( $d\rho/dT > 0$ ) is observed over a narrow temperature range just below the FM transition temperature ( $T_c$ ) and at low temperatures a charge localized state dominates conductivity. FM and the metallic ground state appears only above  $x = 0.18$ . Traditionally, all the physics controlling the basic properties of these systems were believed to be included in the DE model. Close to the “optimal doping” region ( $x \sim 0.3-0.4$ ) the DE model explains most of the basic properties of CMR system. However, recent experimental results and theory show that in the so-called “lightly doped” region ( $x \leq 0.18$ ) DE alone cannot explain many interesting features.<sup>2-11</sup> Additional ingredients such as electron-phonon ( $e$ - $p$ ) interaction causing the JT splitting of  $e_g$  levels, and the on-site Coulomb correlation play important roles in this doping regime.

Recently it has been shown from the neutron diffraction study that  $\text{LaMnO}_3$  undergoes a structural phase transition from the orbitally ordered  $O'$ -orthorhombic to orbitally disordered  $O$ -orthorhombic state at  $T_{JT} = 750$  K. Above  $T_{JT}$  the

Mn-O bond lengths become almost isotropic. Zhou and Goodenough<sup>13</sup> investigated temperature dependence of transport and magnetic properties of  $\text{LaMnO}_3$  both above and below  $T_{JT}$ . They observed almost  $T$ -independent metalliclike conductivity with an isotropic ferromagnetic interaction above  $T_{JT}$ . To understand the interplay between magnetic, transport, and structural properties and to decipher the role of different mechanisms in this family of compounds one needs experimental data as a function of hole concentration, temperature, and structural features. Despite intense research activity in this field, there is no detailed resistivity analysis over a wide range of doping and temperature, particularly in the vicinity of structural transition and beyond. In this paper, we report the high-temperature resistivity behavior of  $\text{La}_{1-x}\text{Sr}_x\text{MnO}_3$  ( $0 \leq x \leq 0.15$ ) single crystals both above and below the structural phase transition temperature. We show that both above and below  $T_{JT}$  the conduction mechanism is governed by the hopping of small polarons with the same activation energy. Several important parameters related to the hopping conduction and  $e$ - $p$  coupling have been deduced from the resistivity analysis.

We have grown  $\text{La}_{1-x}\text{Sr}_x\text{MnO}_3$  single crystals by the floating zone method using an image furnace (NEC SC-M15 HD) in a flow of Ar for  $0 \leq x \leq 0.10$  and in air for  $x > 0.10$ . The typical growth rate was 5 mm/h with a speed of rotation 30 rpm. The polycrystalline ceramic rods of several cm in length and about 5 mm in diameter were prepared by reacting high-purity ( $\geq 99.99\%$ )  $\text{La}_2\text{O}_3$ ,  $\text{SrCO}_3$ , and  $\text{Mn}_3\text{O}_4$  in appropriate ratios at high temperatures. For the  $x = 0$  sample all the heat treatments were done in the presence of Ar flow to keep the oxygen stoichiometry close to 3. Both x-ray powder diffraction and Laue photography were used to determine the structure and verify the crystal quality. The high-temperature resistivity was measured in Ar for  $x \leq 0.125$  and in air for  $x > 0.125$  using a homemade apparatus.

The temperature dependence of resistivity ( $\rho$ ) for the  $x = 0$  sample is shown in Fig. 1(a).  $\rho$  shows a sharp decrease of two orders of magnitude at the JT transition temperature  $T_{JT} = 750$  K and the width of the transition is about 2 K. At low temperatures below  $T_{JT}$ , a large hysteresis between the heating and cooling cycles has been observed similar to that reported earlier by Zhou and Goodenough.<sup>13</sup> They suggested

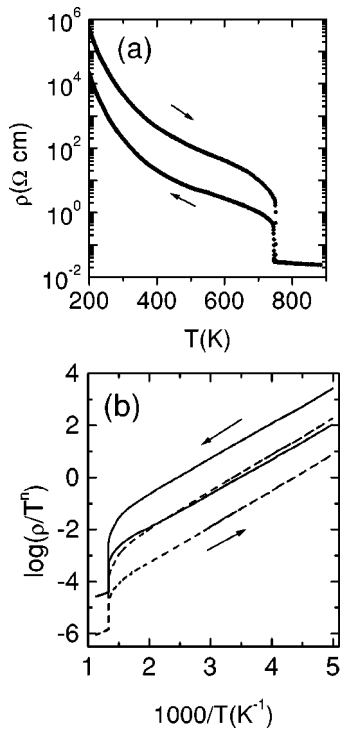


FIG. 1. (a)  $T$  dependence of  $\rho$  for  $\text{LaMnO}_3$  sample. (b)  $\rho$  of the  $\text{LaMnO}_3$  sample plotted in the adiabatic (solid line) and nonadiabatic (dash line) limits.

that this hysteresis may be due to the small oxidation of the sample at high temperatures. From the value of thermopower they estimated that the fraction of  $\text{Mn}^{4+}$  created due to the oxidation is very small ( $<0.001$ ). It has been observed that the hysteresis decreases with the decrease of the highest measuring temperature. This suggests that small oxidation of the sample at high temperature may be the origin of such hysteresis. After a few cycles of heating and cooling the hysteresis becomes negligible. However,  $T_{JT}$  is unaffected by thermal recycling. In the orbitally disordered  $O$ -orthorhombic phase above  $T_{JT}$ ,  $\rho$  is almost temperature independent and shows no hysteresis between heating and cooling cycles. Zhou and Goodenough suggested that this peculiar conductive phase with nearly  $T$ -independent  $\rho$  and isotropic ferromagnetic interaction above  $T_{JT}$  is due to the charge transport by the vibronic carriers.<sup>13</sup> In manganites “small polarons” are formed and at high temperatures they hop from site to site.<sup>14</sup> In the case of small-polaronic conduction the resistivity is given by<sup>14–16</sup>

$$\rho(T) = \rho_0 \exp(E_p/kT) = \frac{akT^n}{g_d e^2 \nu_0} \exp(E_p/kT), \quad (1)$$

where  $a$  is the jump distance of the polaron,  $E_p$  is the activation energy of the polaron,  $\nu_0$  is the characteristic phonon frequency of the system, and  $g_d$  is a constant that depends on the lattice structure.  $n=1$  in the case of adiabatic hopping of polarons and for the nonadiabatic case  $n$  is  $3/2$ . To elucidate the nature of charge transport both above and below  $T_{JT}$  we have plotted  $\log(\rho/T)$  and  $\log(\rho/T^{3/2})$  vs  $1/T$  in Fig. 1(b).

From the figure it is clear that in both the cases  $\rho$  shows Arrhenius behavior over a wide range of temperature well below  $T_{JT}$ . However, the data do not fit with the Mott variable-range-hopping expression (not shown). A significant upward curvature is observed in this case. We observed that  $\rho$  can be fitted well with  $n=1$  and  $3/2$  over the same temperature range. The fit is insensitive to the small difference in the  $T$  dependence of the prefactor  $\rho_0$  in Eq. (1). This is due to the presence of the exponential temperature-dependent factor with large  $E_p$ . However, an indication about the nature of hopping as to whether it is adiabatic or nonadiabatic, may be obtained from the value of  $\rho_0$ . The hopping is termed as adiabatic when the prefactor  $\rho_0$  approaches to the value  $1.43 \times 10^{-3} \Omega \text{ cm}$  at  $kT = h\nu_0$  and it is nonadiabatic if  $\rho_0$  is much larger than this critical value.<sup>14</sup> The values of  $\rho_0$  are  $0.12$  and  $2.0 \Omega \text{ cm}$  at  $300 \text{ K}$  with  $n=1$  and  $3/2$ , respectively. Such a large value of  $\rho_0$  suggests nonadiabatic hopping of polarons. This behavior is different from that observed in the case of the Gd-doped  $(\text{La}_{1-x}\text{Gd}_x)_{2/3}\text{Ca}_{1/3}\text{MnO}_3$  (LCMO) system where the hopping is adiabatic due to the much smaller value of  $\rho_0$ .<sup>14</sup> The value of activation energy  $E_p$  calculated from the linear part of the  $\log(\rho/T^{3/2}) - 1/T$  curve below  $T_{JT}$  is about  $0.3 \text{ eV}$ , which is two to three times larger than that found in other manganites close to the optimum doping  $x \sim 0.3$ .<sup>14,17,18</sup> The adiabatic value of  $E_p$  is about 5% smaller than this. The slope of  $\log(\rho/T^n)$  vs  $1/T$  in the linear region in Fig. 1(b) is the same for heating and cooling cycles. This suggests that in the orbital ordering state and far away from  $T_{JT}$ , the oxygen content in the sample does not change during the measurements.  $g_d$  in Eq. (1) is 1 for nearest-neighbor hopping of polarons. The value of  $g_d$  can be larger if the next-nearest-neighbor hopping probability is significant.<sup>14</sup> Jaime *et al.*<sup>14</sup> used the Mn-O-Mn spacing ( $3.9 \text{ \AA}$ ) as the jump length in the LCMO system to analyze the resistivity data. If we take Mn-O-Mn spacing as the hopping length  $a$  and  $g_d=1$  in these Sr-doped samples then the value of  $\nu_0$  is  $\sim 2 \times 10^{11} \text{ Hz}$  at  $300 \text{ K}$  in the heating cycle which is about two orders of magnitude smaller than the phonon frequency calculated for the LCMO system and the Raman shift of  $\sim 600 \text{ cm}^{-1}$  for optical Mn-O modes.

Although the width of the JT transition is small a systematic deviation from the linear behavior in the  $\log(\rho/T^n) - 1/T$  curve starts at temperatures well below  $T_{JT}$ . The deviation from linearity increases as one approaches towards  $T_{JT}$ . The large downward curvature in the vicinity of  $T_{JT}$  and below suggests an excess conductivity appears. The origin of such excess conductivity may arise from the local Mn-O bond fluctuations. In the orbitally ordered state Mn-O bonds are highly anisotropic due to JT interaction. Though the mean Mn-O bond length changes little with increasing temperature, the orthorhombic distortion changes significantly in the vicinity of  $T_{JT}$ .<sup>12</sup>

In the case of hopping transport the activation energy contains three parts: hopping energy ( $W_H$ ) of polarons and the activation energy due to the disorder ( $W_D$ ) and the polaron bandwidth ( $W_B$ ).<sup>16</sup> At high temperatures and in the nonadiabatic limit the contributions from  $W_D$  and  $W_B$  may be neglected and the polaron binding energy is given by  $W$

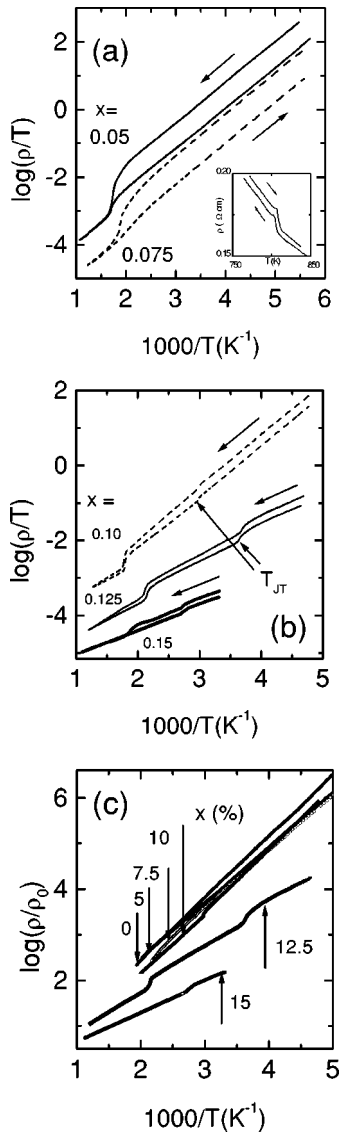


FIG. 2.  $\rho$  of the  $\text{La}_{1-x}\text{Sr}_x\text{MnO}_3$  samples plotted in the adiabatic limit for different  $x$ : (a)  $x=0.05$  and  $0.075$ , (b)  $x=0.10, 0.125$  and  $0.15$ , (c)  $x=0$  to  $0.15$ .  $\rho$  for  $x=0.10$  and  $0.125$  samples in (b) has been shifted upwards by 2 and 1 units, respectively. Inset: The anomalous behavior of  $\rho(T)$  in the vicinity of  $O$ -orthorhombic to rhombohedral structural phase transition ( $T_{OR}$ ) for the  $x=0.05$  sample. In (c)  $\rho$  has been scaled by the prefactor  $\rho_0$  in Eq. (1).

$=2W_H \sim 2E_\rho = 0.6$  eV. The large value of polaron binding energy also indicates small-polaron hopping. Normally, polaron binding energy is calculated using the hopping energy from the Hall mobility. According to the theory the hopping energy in the Hall mobility is about  $2/3$  the conductivity activation energy.<sup>15</sup> In LCMO an excellent agreement between theoretical prediction and experiment has been reported.<sup>14</sup> If this prediction works for other manganites and with different doping levels then the value of  $W$  reduces to  $0.4$  eV which is comparable with polaron binding energy in transitional metal oxides.<sup>16</sup>

In Figs. 2(a) and 2(b) we plot  $\log(\rho/T)$  vs  $1/T$  for  $x \geq 0.05$  samples. Similar to  $x=0$  these samples show a hysteresis between the heating and cooling cycles. In contrast to

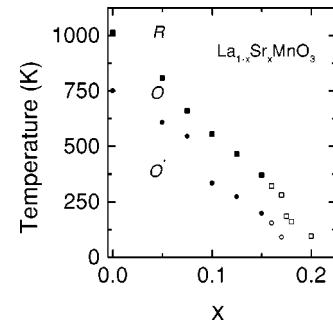


FIG. 3. The temperatures,  $T_{JT}$  and  $T_{OR}$ , where  $\rho-T$  shows an anomaly due to the structural phase transitions (see text) are plotted as a function of doping  $x$  (solid symbols). For  $x > 0.15$  the data have been taken from Refs. 2, 4, and 7 (open symbols).

the pure system, however, a weak hysteresis has been observed in the high-temperature orbital disordered phase and becomes reversible after thermal recycling. Thus unlike the pure system the orbital disordered state for  $x > 0$  samples is sensitive to a small change in the oxidation state of the Mn ion. It is also evident from these figures that  $\rho$  is not  $T$  independent in this high-temperature region. In fact we observe that the slope of the  $\log(\rho/T)-1/T$  curve at high temperatures is almost same as that in the low-temperature region. This suggests the same transport mechanism both above and below  $T_{JT}$ . Thus the presence of  $\text{Mn}^{4+}$  has a dramatic effect on the charge transport mechanism above  $T_{JT}$ . Also the sharpness of the transition is reduced considerably due the presence of  $\text{Mn}^{4+}$  ions. One can compare this behavior with the broadening of the magnetization vs temperature curve of a ferromagnet close to  $T_c$  in the presence of external magnetic field. The FM transition temperature and the anomaly in resistivity around  $T_c$  for  $x \geq 0.10$  are similar to that reported earlier.<sup>2,6,7,19</sup> For  $x=0.05$  and  $0.075$  samples  $\rho$  shows anomaly both at  $T_{JT}$  and around the orthorhombic to rhombohedral structural phase transition temperature ( $T_{OR}$ ) but the anomaly is much weaker in the later case [Fig. 2(a)]. Beside the usual anomaly at  $T_{OR}=370$  K an additional feature appears in  $\rho$  at around  $500$  K in the heating cycle for the  $x=0.15$  sample. Though we do not know its origin, this behavior has also been observed in other samples taken from the different parts of the same crystal. The same slope of  $\log(\rho/T)$  vs  $1/T$  both above and below  $T_{JT}/T_{OR}$  suggests that  $\rho_0$  is scaled on crossing  $T_{JT}$  and  $T_{OR}$ . Another remarkable feature is that the activation energy for the samples  $x \leq 0.10$  is close to  $0.3$  eV as that for  $\text{LaMnO}_3$  but decreases above  $x=0.10$ . This is evident from the  $\log(\rho/\rho_0)$  vs  $1/T$  plot in Fig. 2(c). Though all the curves for  $x \leq 0.10$  do not collapse onto a single curve the dispersion is quite small. Thus the large increase of conductivity with increasing  $x$  does not affect  $E_\rho$  but  $\rho_0$  decreases rapidly.

In Fig. 3 we plot the variation of structural phase transition temperatures  $T_{JT}$  and  $T_{OR}$  determined from the resistivity anomaly as a function of  $x$  along with the data from previous reports<sup>2,4,7</sup> for  $x > 0.15$  samples. Both  $T_{JT}$  and  $T_{OR}$  decrease with increasing  $x$ .  $T_{JT}$  shows a small but sharp drop at around  $x=0.10$  where the system becomes ferromagnetic. In the vicinity of the insulator to metal transition,  $x=0.18$ , a

similar feature has been observed for  $T_{OR}$ . For  $x=0$  and 0.10–0.15 samples the structural phase transition temperatures determined from the resistivity measurements are in good agreement with earlier reports.<sup>2,6,7,12,13</sup> Dabrowski *et al.*<sup>7</sup> investigated the relationship among transport, magnetic, and structural properties in the  $\text{La}_{1-x}\text{Sr}_x\text{MnO}_3$  system for  $0.10 \leq x \leq 0.20$  over a close range of  $x$  and found that above  $x=0.145$  the coherent JT distortion is suppressed by the long range FM ordering but the incoherent JT distortion increases initially and then decreases as the system becomes metallic close to  $x=0.18$ .

In conventional BCS superconductors the ratio of energy gap ( $2\Delta$ ) and superconducting transition temperature is a measure of electron-phonon interaction strength. Similarly in the case of collective excitation such as charge density wave (CDW) and spin density wave (SDW) ordering the ratio of energy gap and transition temperature defines the strength of interaction. We do not know much about the order parameter of the orbital ordering, but similar to superconductivity, CDW, and SDW, we can define the ratio  $2\Delta_{JT}/kT_{JT}$ , where  $2\Delta_{JT}$  is the energy gap between the two  $e_g$  orbitals due to the cooperative JT interaction, as a strength of the interaction

between electron and JT phonon. This ratio is about 9 for the  $x=0$  sample if we assume  $2\Delta_{JT}=0.6$  eV. The strength of  $e$ - $p$  interaction can also be estimated from the polaron binding energy ( $W$ ). In the case of hopping of polarons the ratio  $\gamma=W/hv_0$  defines  $e$ - $p$  coupling strength.<sup>16</sup> If we assume the Raman shift of  $\sim 600$   $\text{cm}^{-1}$  for optical Mn-O vibration then  $\gamma \sim 7.5$ . This value is typical for small-polaronic conduction.

In conclusion, we have analyzed the  $T$  dependence of  $\rho$  over a wide temperature range for the lightly doped insulating system  $\text{La}_{1-x}\text{Sr}_x\text{MnO}_3$  with  $0 \leq x \leq 0.15$ . Except for the  $x=0$  sample, the electrical conduction is dominated by the hopping of small polarons both above and below  $T_{JT}$  with the same activation energy. The  $x=0$  sample shows hopping conduction only in the orbitally ordered phase but  $\rho$  is almost  $T$  independent above  $T_{JT}$ . Though the conductivity increases dramatically with Sr doping,  $E_\rho$  remains independent of  $x$  up to  $x=0.10$  and then decreases with further increase of  $x$ . Our results show that the electron-phonon coupling plays an important role in the lightly doped regime.

We are grateful to A. K. Pal for technical help during the measurements at high temperatures.

<sup>1</sup>E.O. Wollan and W.C. Koehler, Phys. Rev. **100**, 545 (1955).

<sup>2</sup>A. Urushibara, Y. Moritomo, T. Arima, A. Asamitsu, G. Kido, and Y. Tokura, Phys. Rev. B **51**, 14 103 (1995).

<sup>3</sup>Y. Yamada, O. Hino, S. Nohdo, R. Kanao, T. Inami, and S. Katano, Phys. Rev. Lett. **77**, 904 (1996).

<sup>4</sup>Y. Moritomo, A. Asamitsu, and Y. Tokura, Phys. Rev. B **56**, 12 190 (1997).

<sup>5</sup>Y. Endoh, K. Hirota, S. Ishihara, S. Okamoto, Y. Murakami, A. Nishizawa, T. Fukuda, H. Kimura, H. Nojiri, K. Kaneko, and S. Maekawa, Phys. Rev. Lett. **82**, 4328 (1999).

<sup>6</sup>S. Uhlenbruck, R. Teipen, R. Klingeler, B. Büchner, O. Friedt, M. Hücker, H. Kierspel, T. Niemöller, L. Pinsard, A. Revcolevschi, and R. Gross, Phys. Rev. Lett. **82**, 185 (1999).

<sup>7</sup>B. Dabrowski, X. Xiong, Z. Bukowski, R. Dybzinski, P.W. Klamut, J.E. Siewenie, O. Chmaissem, J. Shaffer, C.W. Kimball, J.D. Jorgensen, and S. Short, Phys. Rev. B **60**, 7006 (1999).

<sup>8</sup>H. Kawano, R. Kajimoto, M. Kubota, and H. Yoshizawa, Phys. Rev. B **53**, 709 (1996).

<sup>9</sup>A.J. Millis, P.B. Littlewood, and B.I. Shraiman, Phys. Rev. Lett. **74**, 5144 (1995).

<sup>10</sup>H. Röder, J. Zang, and A.R. Bishop, Phys. Rev. Lett. **76**, 1356 (1996).

<sup>11</sup>I. Solov'yev, N. Hamada, and K. Terakura, Phys. Rev. Lett. **76**, 4825 (1996).

<sup>12</sup>J. Rodriguez-Carvajal, M. Hennion, F. Moussa, A. Moudden, L. Pinsard, and A. Revcolevschi, Phys. Rev. B **57**, R3189 (1998).

<sup>13</sup>J.-S. Zhou and J.B. Goodenough, Phys. Rev. B **60**, R15 002 (1999).

<sup>14</sup>M. Jaime, H.T. Hardner, M.B. Salamon, M. Rubinstein, P. Dorsey, and D. Emin, Phys. Rev. Lett. **78**, 951 (1997).

<sup>15</sup>D. Emin, and T. Holstein, Ann. Phys. (N.Y.) **53**, 439 (1969).

<sup>16</sup>I.G. Austin and N.F. Mott, Adv. Phys. **18**, 41 (1969).

<sup>17</sup>M. Jaime, M.B. Salamon, M. Rubinstein, R. Treece, J. Horwitz, and D.B. Chrisey, Phys. Rev. B **54**, 11 914 (1996).

<sup>18</sup>D.C. Worledge, G.J. Snyder, M.R. Beasley, T.H. Geballe, R. Hiskes, and S. DiCarolis, J. Appl. Phys. **80**, 5158 (1996).

<sup>19</sup>A. Anane, C. Dupas, K. Le dang, J.P. Renard, P. Veillet, A.M. de Leon Guevara, F. Millot, L. Pinsard, and A. Revcolevschi, J. Phys.: Condens. Matter **7**, 7015 (1995).